JTTEE5 15:198-205
DOI: 10.1361/105996306X108048
1059-9630/$19.00 © ASM International

Peer Reviewed

Air Gas Dynamic Spraying of Powder Mixtures: Theory and Application

R. Gr. Maev and V. Leshchynsky

(Submitted August 25, 2005; in revised form January 16, 2006)

The radial injection gas dynamic spray (RIGDS) technology of powder coatings deposition was considered for this work. A coating was created by injecting powders with variable compositions into a supersonic air jet and depositing powder on the substrate. This study describes the preliminary analysis of an air gas dynamic spray method realized by a portable RIGDS apparatus with a radial injection of powder. Attention was given to shock compaction processes during the coating structure formation and examples of powder mixtures utilization in RIGDS. It was shown that the operational parameters of supersonic powder-gas jet have a significant influence on the coating's microstructure, thus defining the high performance of the coating. Compaction and bonding of particles were analyzed.

Keywords cold gas dynamic spraying, composite materials, influence of spray parameters, properties of coatings

1. Introduction

Gas dynamic spraying (GDS) is a new coating deposition technology, which is being developed to produce high quality metallic coatings (Ref 1-12). The GDS process is based on exposing a substrate to high velocity solid-phase particles accelerated by a supersonic gas flow at a temperature lower than the melting point of the particles. The low-temperature nature of GDS makes it possible to deposit coatings of powder materials without any considerable changes in the microstructure of the feedstock. Many metals, such as Cu, Al, Ti, and their alloys, have been deposited by GDS (Ref 1-8). Even some cermets (Ref 9) and ceramic particles (Ref 2) were embedded into a metallic substrate to form a thin layer coating. However, the application of powder metal-ceramic mixtures for GDS and the analysis of their effect on at GDS process have not been deeply studied yet.

It is already a known fact that coatings in GDS are formed due to significant plastic deformation of both the sprayed particles and the substrate, caused by impacts of the accelerated particles. The high-impact pressures result in the direct contact of pure metals through breakup and dispersion of the thin oxide film on both particle and substrate surfaces providing creation of strong metallic bonds (Ref 3). On the other hand, the intensive deformation of the particle and substrate results in the high strain and temperature rise at the localized contact areas. Several numerical simulation studies have indicated that the temperature at the contact zone, caused by the adiabatic shear during deposition, can reach a value near the melting point of the sprayed materials and a thin melted layer could be formed (Ref 5, 6). Based on the metallic jetting observed with the impact of cold sprayed $TiAl_6V_4$ particles, Vlcek et al. (Ref 2) suggested that this jetting resulted from the occurrence of melting at the impacting interface. However, the occurrence of jetting may be a result of localized deformation in the interface area under dynamic loading (Ref 13). Additionally, strain localization may occur not only at the interface. Adiabatic shear bands may also occur in bulk particles (Ref 14) as well as in powder granular media (Ref 15). The lack of strain localization analysis, and particularly its influence on the structure of the formed coatings, limits the present understanding of the deposition mechanism in the GDS process.

Because the common approach to GDS coating formation is based on the analysis of the interaction between a single particle and a substrate, it is rather important to study adiabatic shear bonding processes in powder layers, taking into account the structure of the granular media, i.e., particle ensembles. In the present approach, the attempt was to combine the theory of fluid mechanics relevant to solid particles suspended in a supersonic gas stream with the theory of particle consolidation during the spraying process. If the air-particle jet consists of particles of various sizes then the nature of the particle interaction and coating formation depends on the behavior of particle ensembles upon impingement (Ref 16).

The basis of the current GDS technology is to create a very high speed gas that can accelerate the injected powders to velocities above critical (about 500-800 m/s). This is normally achieved by expanding helium or nitrogen in a Laval nozzle. The pressure ratio for this expansion is in the order of 23. Because of its light weight, helium is a much better gas to work with. It is however very expensive and makes the use of the process in an industrial environment economically unfeasible. The critical gas velocity is material dependant and is affected by the density and elastic-plastic properties of the material, particle size, and powder composition (Ref 5, 17). The authors (Ref 18) have shown that the critical velocity for GDS of Al based powders accelerated by air was in the range of 400-500 m/s. Moreover, the application of relatively large particles in the air GDS process allows us to reach the kinetic energy necessary to realize their

The original version of this paper was published in the CD ROM *Thermal Spray Connects: Explore Its Surfacing Potential,* International Thermal Spray Conference, sponsored by DVS, ASM International, and IIW International Institute of Welding, Basel, Switzerland, May 2-4, 2005, DVS-Verlag GmbH, Düsseldorf, Germany.

R. Gr. Maev and **V. Leshchynsky,** University of Windsor, Windsor, Canada. Contact e-mail: leshnysk@uwindsor.ca; maev@uwindsor.ca.

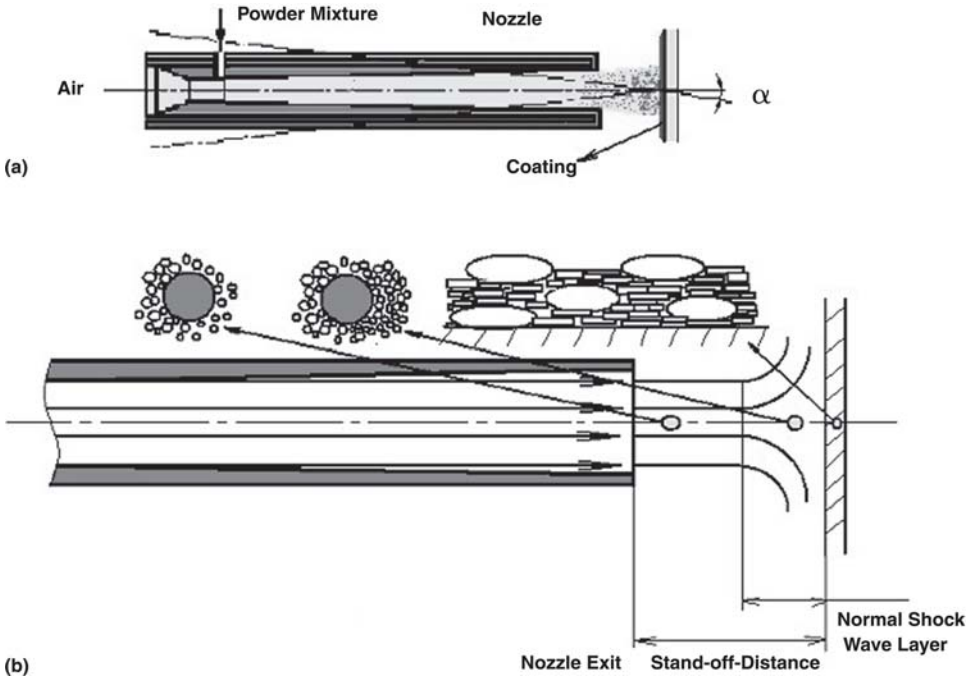

Fig. 1 Composite coating structure formation model for spraying powder mixture: (a) general scheme of powder jet and coating and (b) particle arrangement in powder jet

deformation and bonding with low particle critical velocities [air GDS process referred to as kinetic spray (Ref 18)]. In the case of Mach numbers 1.2-2, an air pressure ratio is calculated to be in the range of 2.4-7.8. Thus, to achieve the critical particle velocities with the air stream, it is possible to apply the GDS systems with air pressure parameters of about 5-8 bars.

Radial injection of the powder is one of the main advantages of the radial injection gas dynamic spray (RIGDS) technology due to the high durability of the nozzles and simple design of the powder hoppers (Ref 19). The low air pressure and radial injection of the powder leads to decreased gas consumption and sharply improves the economical feasibility of the RIGDS process for the industrial environment.

Thus, the purpose of this study is to encourage further understanding of the role of the powder radial injection in structure formation during the spraying powder mixtures.

2. Experimental Procedure

The spraying of Al-based powder mixtures on steel and aluminum substrates was performed by an apparatus incorporating the DYMET (SST Centerline, Windsor, Canada) gun (Ref 19) with the injection of powder into the divergent part of a supersonic nozzle. The schematic of the spray process is shown on Fig. 1.

The powder mixtures were supplied by a powder hopper and injected into the supersonic portion of the nozzle near the throat area by means of negative pressure developed by the accelerated stream of compressed air passing through the nozzle. The injected particles are accelerated in the high-velocity air stream by the drag effect. To increase the air velocity and, ultimately the particle velocity, the compressed air can be preheated within a range from 100 to 700 °C. The pressure and the temperature of the compressed air were monitored by a pressure gage and a thermocouple positioned inside of the gun. The gun was installed on an X-Y manipulator to drive the air-powder jet over the substrate surface. The compressed air pressure was kept constant at 0.5 MPa. It is important to note that the air pressure was essentially lower than in other GDS systems [usually in the range of 2.0 to 5 MPa (Ref 1-4)]. This feature makes GDS with DYMET gun much more suitable for the industrial environment because a special high pressure pump is no longer needed. However, the air consumption is lower as well, about 0.2-0.3 m^3/min as compared with 1.3 m^3/min for spray systems using an axial injection of powder (Ref 2). The particle velocities at the exit of the supersonic nozzle were in the range of 550 m/s, as measured by laser doppler velocimeter. The powder feeding rate varied in the range of 0.5-1.5 g/s, while the standoff distance from the exit of the nozzle to the substrate was held constant at 10 mm. A rectangular nozzle with an exit aperture of 3.5 × 10 mm was used.

Commercially available aluminum powder (−300 mesh), zinc powder (5-10 μm), and tungsten powder (3-10 μm) were used as base materials. The Al powder used for coating deposition was sieved to sizes ranging from 40 to 60 μm to limit the effect of particle size distribution. The scanning electron microscope (SEM) images of the powders used are shown in Fig. 2. Mild steel and Al were used as substrates. Prior to spraying, the substrate surface was sandblasted using 300 mesh alumina grits. Two component Al-Zn and three component (W-Al-Zn and Ti-Al-Zn) powder mixtures were used in the experiments. The deposition efficiency of GDS was measured on grit blasted 3 mm thick aluminum substrates. The substrates were cleaned with acetone and methanol, dried in hot air and weighed before and after processing. The portion of the powder mixture of 25 g for one sample was weighed as well.

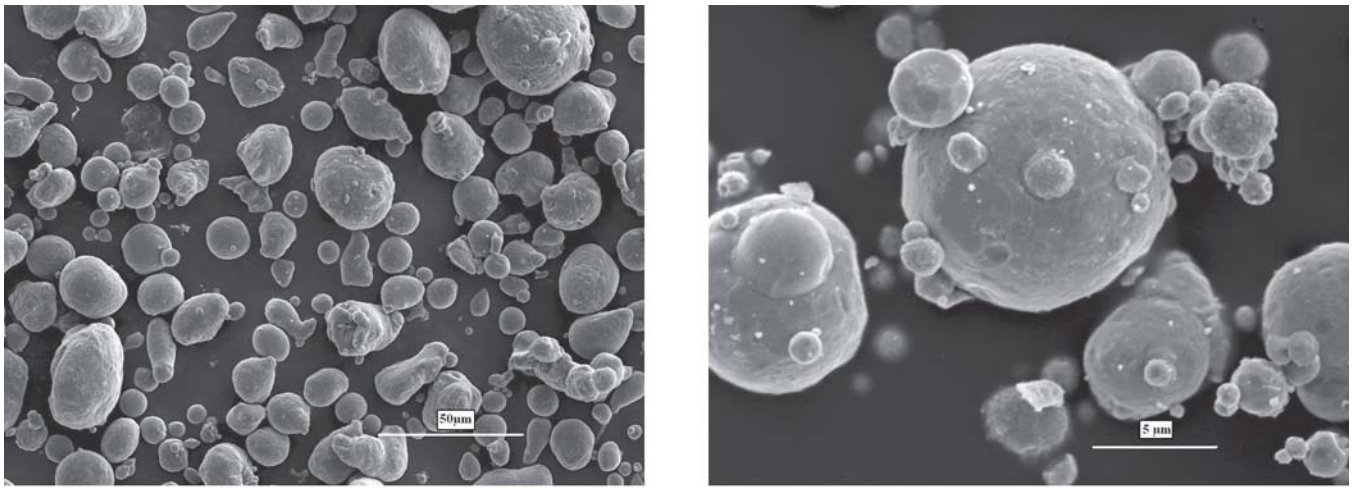

Fig. 2 SEM images of base powders for powder mixtures: (a) Al powder (×500) and (b) Zn powder (×5000)

Characterization of the coatings is based on microhardness measurements. The coating structure was examined using Light Microscope after polishing and 10 s etching with Tucker's reagent. The phases of the coating were identified by x-ray diffraction (XRD).

3. Results

The GDS experimental results are analyzed with respect to the effects of air temperature T_g, powder jet composition, powder jet incidence angle α and stand-off-distance x_d. The air temperature influences the air and particle velocity, which are to be as high as possible. However, optimization of particle interaction and bonding during the spraying process may be achieved through the intensification of particle deformation and interparticle sliding. These processes are controlled through the composition of the powder impinging the substrate, particle sizes, and an incidence angle. In an effort to better understand the process, the following dependences are to be examined:

- deposition efficiency versus air temperature (Fig. 3) and powder feeding rate (Fig. 4)
- average single pass thickness of deposited layer versus air temperature (Fig. 5)
- hardness versus depth from the surface (Fig. 6)

Experimental results demonstrate some features of powder mixtures sprayed at low air pressures. Deposition efficiency χ_D of GDS is found to be low in the range of temperatures 100-500 °C, but sharply increases at temperatures higher than 600 °C and becomes comparable with the values of χ_D for Ti and Cu (Ref 17). It is important to note that nitrogen was applied for GDS of Ti (Ref 8) and copper (Ref 4). It is known that the nitrogen and helium propellant gases allow us to achieve higher gas and particle velocities than air (Ref 20). Particle velocities reach critical values at a temperature of 300 °C for nitrogen. The deposition efficiency of Ti is above 0.6 at this temperature (Fig. 3) (Ref 8). For air GDS at a low pressure of 0.5 MPa, the χ_D value ~0.6 is realized at air temperatures of 650 °C. Thus, it can be assumed

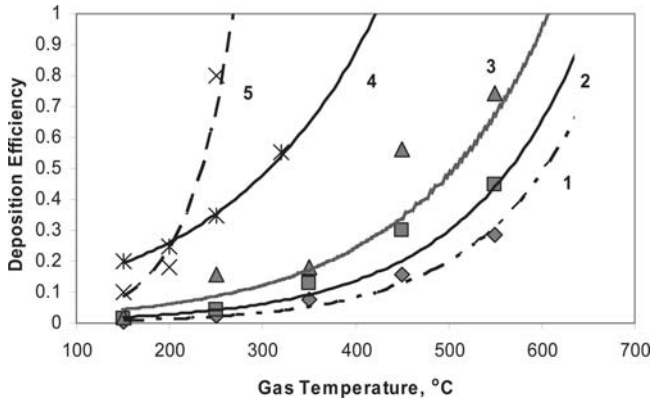

Fig. 3 Deposition efficiency for powder mixtures: (1) Powder mixture with weight concentration $0.25Al_2O_3$ + 0.5Al + 0.25Zn, (2) Powder mixture with weight concentration 0.5Ti + 0.25Al + 0.25Zn, (3) Powder mixture with weight concentration 0.5W + 0.25Al + 0.25Zn, (4) Cu (4), and (5) Ti (8).

that the critical velocity threshold of 500 m/s (Ref 20) is achieved at this temperature.

The dependence of deposition efficiency from temperature is accurately described by an exponential approximation for all powders and powder mixtures (Fig. 3). Simulation veracity is in the range of R^2 = 0.94 to 0.99. The deposition efficiency equation is approximated by:

$$\chi_D = \chi_{D_o} e^{-Q_D/RT_0} \quad \text{(Eq 1)}$$

where χ_{Do} is exponent coefficient and Q is activation constant of the GDS process.

Approximations of the experimental data for powder mixtures studied are shown in the next table for three types of powder mixtures.

Analysis of constants of Eq 1 show that the values of χ_{Do} do not vary for powder mixtures 1-3, while the values of Q_D are

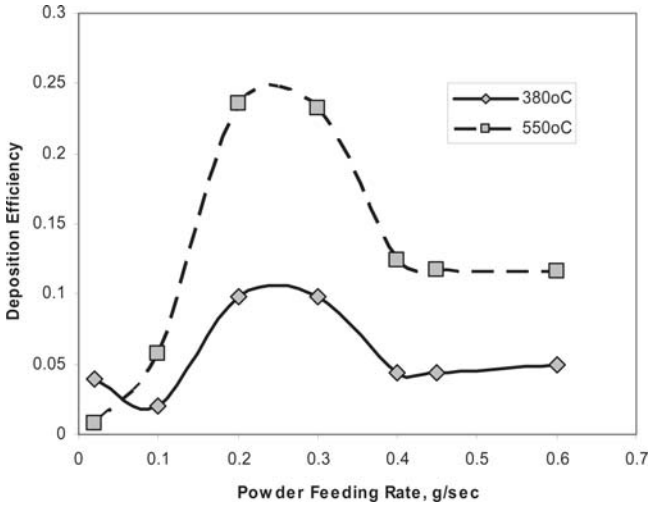

Fig. 4 Deposition efficiency versus powder feeding rate. Experimental data for Al-based powder mixture with weight concentration $0.25Al_2O_3 + 0.5Al + 0.25Zn$

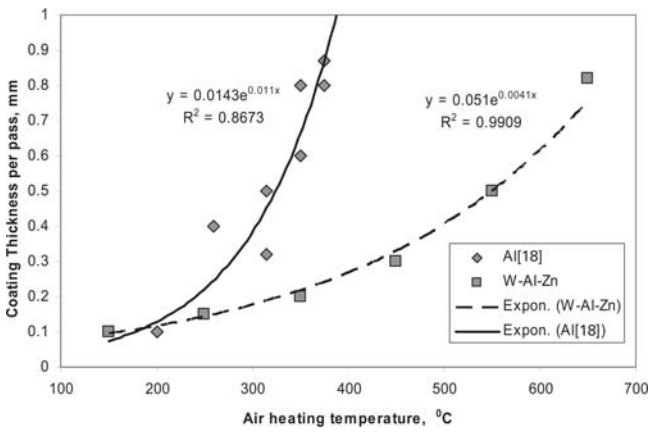

Fig. 5 Average single pass thickness–air temperature dependence; experimental data and exponent approximations for Al (Ref 18) and Al based powder mixture with weight concentration 0.5W + 0.25Al + 0.25Zn

slightly different. This means that critical particle velocity, defined by the gas temperature, is the same for all powder mixtures studied because they consist of Al and Zn particles, which are deformed during impact with substrate and coating forming. The values of the activation constants reveal to some extent the kinetic parameters of a powder build up process, which depends on the type and volume concentration of big and heavy particles. Thus, the deposition efficiency of the powder mixture 3 (Table 1) is high due to higher kinetic energy of tungsten heavy particles, resulting in the conversion of plastic work into heat and stored energy in the formed GDS coating.

The effect of the particle mass flow rate M_s on the deposition efficiency is shown on Fig. 4. The maximum of function $\chi_D = \chi_D(M_s)$ reveals that there is an optimal value of particle mass flow rate, which provides an optimal concentration of particles in the powder jet. It is characterized by μ, the particle-to-gas mass flow ratio, $\mu = M_s/M$, where M is the gas mass flow rate. If the air

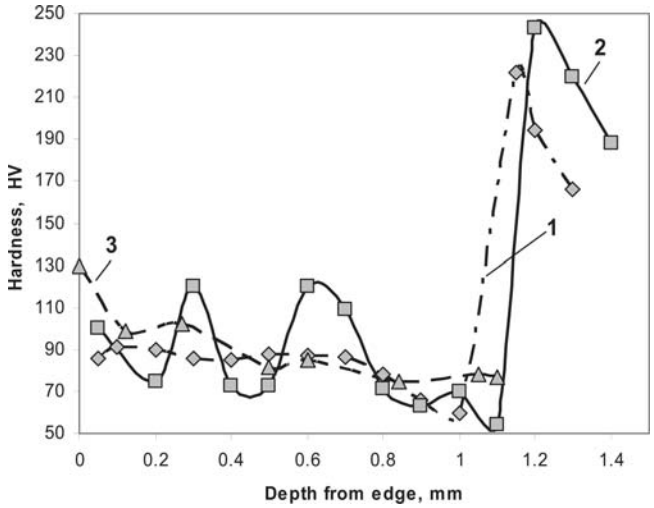

Fig. 6 Micro-hardness $HV_{0.1}$ versus depth of coating: (1) Al-Ti-Zn coating, (2) Al-W-Zn coating, and (3) Al coating (Ref 14)

temperature in the nozzle outlet area is about 200 °C (Ref 18) and air density is $\rho = 0.746$ kg/m^3, then particle-to-gas mass flow ratio μ depends on the particle mass flow rate M_s. It is within the range of $\mu = 0.035$ to 0.3. The optimal value of μ for which the deposition efficiency is maximal is approximately $\mu = 0.27$. The particle-to-gas mass flow ratio for a kinetic spray process (Ref 18) is about $\mu = 0.06$. Despite lower powder feeding rates in the case with the DYMET gun (as compared with the usual GDS process with axial powder feeding), it reached a higher concentration of solid phase in the powder-laden jet by approximately five times. The main reason for the specific shape of function $\chi_D = \chi_D(M_s)$ is believed to be due to the influence of the normal shock wave layer with a higher concentration of powder particles. The particles rebound from the substrate surface and collide with the particles from the powder jet, sharply decreasing their kinetic energy. Therefore, the particles with reduced kinetic energy are no longer able to consolidate and form a coating. It has to be noted that the χ_D maximum occurs on all curves for different air temperatures (Fig. 4) despite the low particle velocities corresponding to low air temperatures. This means that some particles reach the velocity threshold needed to create bonding. The mechanisms of such particle behavior, however, are currently unclear.

The average single pass thickness of a GDS coated layer, t, is one of the main parameters characterizing GDS build up capability. Its dependence on air temperature is shown on Fig. 5. The semiempirical relationship, which gives a good approximation of the experimental data, is similar to Eq 1:

$$t = t_o e^{-Q_t/RT_0} \quad \text{(Eq 2)}$$

The parameters t and Q_t of Eq 2 are shown in Table 1. It can be seen that activation constant Q_t does not depend on the air temperature and, consequently, particle velocity. At the same time the parameter t increases by about two times showing the influence of the powder composition on the build up process. The comparison of the activation constants in Eq 2 reveals the same order of magnitude. These expressions, describing the de-

position efficiency and average single pass thickness parameters by means of an exponential function, correctly reflect the behavior of certain physical parameters. For a deeper understanding of GDS physical mechanism it is necessary to develop new phenomenological models that would include the interaction of particles during GDS deposition of powder mixtures.

The microstructure of composite coatings deposited by GDS and the examination of their properties reveals some important features of composite layer formation (Fig. 7). First, the structure of two-component coating, made of 0.45 Al and 0.55 Zn volume ratios, consists of large Al particles surrounded by small Zn particles. Second, the number of Zn particles located between Al particles is only about 5-10% and the concentration of Zn in the composite coating is about 30-40%, as evaluated from the microstructure. The collision frequency of small particles, however, is much higher than that of large Al particles due to a higher concentration of Zn particles in the powder jet. This data indicates that a more intensive rebound of Zn particles than Al particles is taking place during powder jet-substrate interaction. This conclusion was verified by an additional microstructure examination of Al-Zn powder mixtures with different concentrations. The Al and Zn particles exhibit different rebound ability depending on the particle velocity and the air temperature. So, the final content of Al and Zn phases in coatings does not match initial composition in the powder jet. The loss of Zn content up to 15% was observed at an air temperature of 550 °C. The obtained data shows the great importance of the rebound process occurring during the interaction between powder laden jet and the substrate.

The main principle governing the formation of GDS coatings relates to the extensive plastic deformation at the particle-substrate interface (Ref 11) due to the localization of deformation during particle impact with the substrate. As stated by a number of authors (Ref 2-11), the bonding mechanisms in GDS can be similar to shock compaction. The shock compaction of particle mixtures is very likely to be realized during GDS of powder mixtures. From this viewpoint, the choice of powder compositions with optimized consolidation properties for GDS technology is of great importance. The construction of such powder mixtures is believed to be based on:

- optimization of shock consolidation of powder mixtures by the incorporation of heavy and large particles into the powder jet
- choice of the particles with high density as they penetrate to powder mixtures
- solid phase reactions to influence a proper bonding of particles

For this reason, the authors examined the microstructure of two component Al-Zn coatings and three component Ti-Al-Zn (Fig. 7a) and W-Al-Zn (Fig. 7b) coatings. The processes of structure formation result in different hardness of the deposited coatings (Fig. 6). The distribution of hardness is relatively uniform for

Table 1 Parameters of exponential approximations

Number	Powder composition by weight	Exponent coefficient of Eq 1, χ_{D_0}	Activation constant of Eq 1, $Q_{D,kJ/mol}$	Exponent coefficient of Eq 2, t_0	Activation constant of Eq 2, $Q_{t,kJ/mol}$
1	25% A_2O_3 + 50% Al + 25% Zn	21.95	29.07	3.19	12.9
2	50% Ti + 25% Al + 25% Zn	20.35	26.05	4.97	12.92
3	50% W + 25% Al + 25% Zn	21.62	23.4	6.93	12.83
4	Copper (nitrogen) (Ref 4)	6.48	12.45	…	…
5	Titanium (nitrogen) (Ref 8)	4513	37.5	…	…
6	Aluminum (air) (Ref 18)	…	…	164.2	28.47

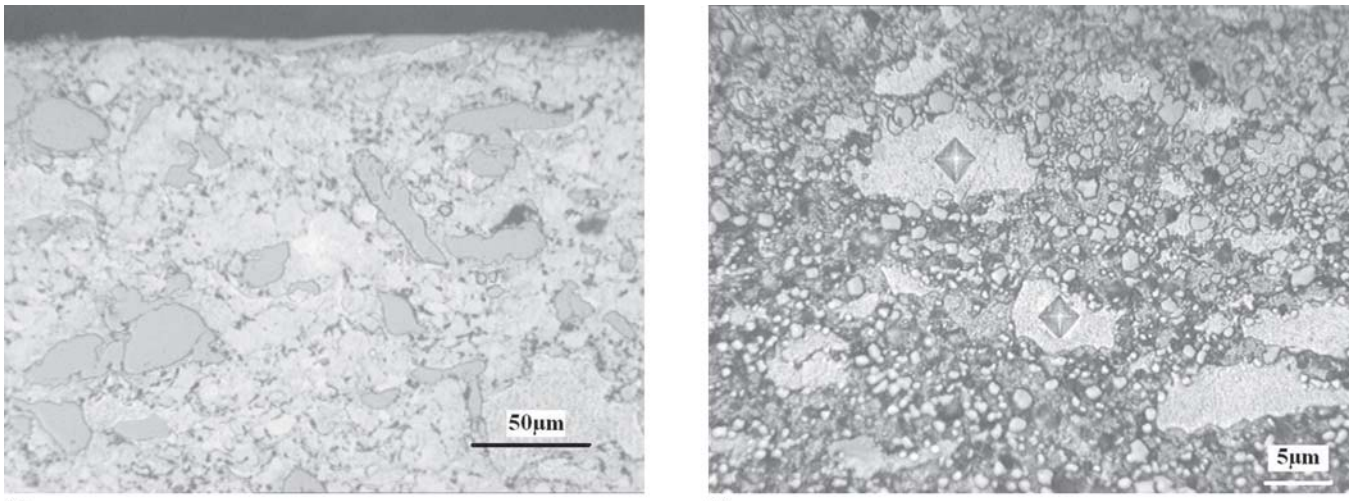

Fig. 7 Structure of composite coatings: (a) Al-Ti-Zn composite coating and (b) Al-W-Zn coating (not etched)

pure aluminum coatings (Ref 21) and composite W-Al-Zn coatings (the scatter is of 5-7 units), while the hardness of Al-Ti-Zn coatings varies in the range of 70-120 $HV_{0.1}$. This is probably a result of mechanical alloying reactions, which may occur during the collision of Al, Zn, and W particles. Additionally, all coatings have a lower hardness in the vicinity of the substrate surface. This phenomenon is believed to be explained by the effect of the localization caused by the severe particle deformation during the deposition process. At the same time, the hardness of the substrate is very high due to the surface strengthening that takes place during the grit blasting process. The phase microhardness examination results reveal the effect of W and Ti on the microhardness of the aluminum phase in the range of 10-20 units, proving the assumption that mechanical alloying reactions occur (Fig. 8).

4. Discussion

Three main issues have to be discussed based upon the experimental data presented in the previous chart: background of Arrhenius law application for phenomenological analysis of GDS process, powder mixtures behavior during GDS, and shear localization and mechanical alloying features of GDS coating structure formation.

An expression of the deposition efficiency and average single pass coating thickness by fitting the Arrhenius equations Eq 1, 2 seems to be reasonable because the gas temperature defines the particle velocity in powder jet with the equation (Ref 20):

$$V_p = (M-1)\sqrt{\frac{\gamma_c RT_0}{1+[(\gamma_c-1)/2]M^2}} \quad \text{(Eq 3)}$$

where T_0 is the initial gas temperature (in convergent part of nozzle), M is Mach number, γ_c is the ratio of specific heats or isentropic coefficient (Ref 17) . For monatomic gases, γ is 1.66, and for diatomic gases γ is typically 1.4. (Air is typically modeled as a diatomic gas because it is a mixture of nitrogen and oxygen). The modeling results and analytic equations shown by Dykhuizen and Smith (Ref 20) based on the isentropic gas flow model were used to make a rough estimation of the particle velocity. The analytical Eq 3 presents a dependence of particle velocity and gas temperature. As the authors (Ref 20) mentioned, this equation may be used to approximately calculate the particle velocity only when the optimal nozzle shape is used. The relationship (Eq 3) does not take into account particle parameters due to some difficulties to obtain the analytical solution of the base equations with the main variables of a drag coefficient, particle density, and size. This equation was used only for rough analysis of particle velocity dependence from the temperature and type of the propellant gas (RT_0).

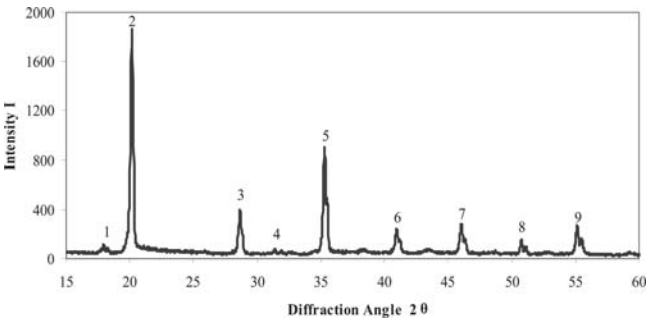

Fig. 8 XRD spectra of Al-W-Zn coating. 1, 3, 8, 9 – $Al_{0.71}Zn_{0.29}$; 2, 4, 5, 6, 7 – WAl_{12}

The collision contact time t_c can be approximated by:

$$t_c \approx \frac{d}{V_p} \quad \text{(Eq 4)}$$

where d is the diameter of the incoming particle. The severe deformation of particles due to impact is described by shear strain γ, which is possible to evaluate roughly from microstructure analysis. In this case, shear strain rate may be calculated as:

$$\dot{\gamma} \approx \frac{\gamma}{t_c} \quad \text{(Eq 5)}$$

One can find RT_0 from Eq 3 as:

$$RT_0 = f(\gamma_c, M)V_p^2, \text{ where } f(\gamma_c, M) = \frac{1+\frac{\gamma_c-1}{2}M^2}{(M-1)^2\gamma_C}$$

Equation 2 is modified taking into account Eq 4 and 5:

$$t = t_0 \exp - \frac{Q_t}{f(\gamma_c, M)d^2\left(\frac{\dot{\gamma}}{\gamma}\right)^2} \quad \text{(Eq 6)}$$

Equation 6 reveals the buildup effectiveness of the GDS process is determined by the relation ($\dot{\gamma}/\gamma$) or by the process of adiabatic shear bands formation at the particle interface. Various materials exhibit narrow bands of intense plastic deformation, termed shear bands, under extreme loading conditions (Ref 14, 22). The thermomechanical mechanism of shear bands formation is associated with shear localization during high strain rate loading in a rate-sensitive materials such as polycrystalline metals (Ref 13, 14, 22, 23) or granular materials (Ref 24). Under this mechanism, thermal softening is thought to overcome hardening effects in the material, and to push forward the shear bands formation process. The flow law with Arrhenius dependence on temperature is used to model shear localization and shear bands phenomena in thermoviscoplastic materials (Ref 13-15, 22). The authors (Ref 25) made the first comprehensive analytical study of shear localization with Arrhenius flow law in one-dimensional formulation on the base of $\dot{\gamma}$ plastic strain-rate function ("flow law") analysis. The strain-rate function $\dot{\gamma}$ depends on temperature and stress. Physically, the nature of the plastic flow governs shear bands formation, and its mathematical representation is the source of nonlinearity in the problem (Ref 25). Theoretical models based on microstructure and the physics of deformation use thermal activation of plastic flow, which leads to an Arrhenius dependence on temperature (Ref 15, 16, 26). Such models are used in numerical studies (Ref 14), but many analytical studies approximate flow laws to simplify the

calculation. In particular, an exponential flow law is often used (Ref 25):

$$\dot{\gamma} = \dot{\gamma}_0 \tau^N e^{-\frac{Q}{RT_D}} \quad \text{(Eq 7)}$$

where T_D is the deformation temperature, Q is an activation energy, N is the power coefficient ($N \geq 0$), τ is the shear stress in the area of shear localization. The main feature of Eq 7 is shear strain rate Arrhenius dependence on temperature. The comparison of Eq 6 and 7 shows that such macroscopic characteristics of the GDS process as the average single pass thickness t or the deposition efficiency χ_D depend on kinetics of the adiabatic shear bands formation, which is described by means of the Arrhenius flow law. The interrelation of Eq 6 and 7 will be further studied to better understand the physics of shear localization as the main coating structure formation process during particles impact loading in GDS.

The detailed analysis of the flow characteristics of gas-particle suspensions in a powder-laden jet seems to be important from the viewpoint of particle-particle collision and particle-turbulence interaction evaluation. These processes were studied both for the diluted (Ref 27) and the concentrated gas-solid suspensions (Ref 28). Despite the relatively high gas velocities (300-900 m/s) in these "fast fluid bed" units (Ref 27), the concentration of suspended solids is not uniform along the nozzle axis, as well as over the cross section of the flow. High particle concentration generally forms near the nozzle walls, near particles moving with low velocity. Clusters of particles may also intermittently form and disintegrate in the diluted suspension flows (Ref 27, 28). Thus, the probability of particle cluster formations may be evaluated by the difference of particle axial velocities ΔV_i. The gradient $\Delta V_{(1\text{-}50)} = V_1 - V_{50}$, where V_1 and V_{50} are the velocities of particles of sizes 1 and 50 μm is about 600 m/s. Even a small difference in particle sizes results in a velocity gradient about 100-200 m/s. The scheme of particle clusters for the case of spraying bimodal powder mixtures is shown in Fig. 1(b). There are two areas of the powder jet: free jet with the length near the stand-off-distance and the normal shock wave layer.

The average concentration of particles rebounding from the substrate is high in the normal shock wave layer. This leads to an increase of particle concentration in clusters moving through the normal shock wave front. Two conclusions can be drawn: velocity of the cluster depends on the particles rebound process and coating formation in the case of particle clusters impingement with a substrate is similar to powder shock compaction.

In this case, the particles with low velocity and high weight, which are the cores of clusters, play the role of shot balls in the powder shock consolidation process (Ref 29). These particles are distributed in the matrix of small particles (Fig. 7). Therefore, the impact powder microforging process is realized. The ratio of the particle sizes, weights, and concentration governs the efficiency of the powder microforging impact, resulting in bonding and densification of powder layers.

An XRD spectrum of Al-W-Zn coating is shown on Fig. 8. After GDS, the observed XRD peaks show new phases, which are a result of deformation enhanced alloying. The mechanical alloying processes are known to develop due to intensive particle deformation during high energy mechanical milling (Ref 23). Thus, it can be assumed that the main reason for the presence of mechanical alloying processes in GDS is the severe deformation of particles and shear localization at the particles' interface (Ref 12).

5. Application

Localized plastic deformation at the particle-substrate interface appears to be necessary for the coating formation. For this reason, successful powders and substrates for GDS are mostly metals with relatively high plasticity. Nevertheless, mixtures of metals and ceramics can be successfully sprayed onto metallic surfaces and conversely, metal powders can be successfully applied to ceramic substrates (Ref 29). Apparently, in the case of low pressure air RIGDS the presence of a metallic component appears to compensate for the lack of ductility of the ceramic component. In general, the range of materials that can be successfully sprayed by RIGDS, include pure metals such as Al, Zn, Cu, Fe, Ni, Ti, and composites such as Al-Al_2O_3, Al-B_4C, Cu-W, etc. Already, air RIGDS has found multiple applications in many industries including aerospace, automotive and rebuild.

The main examples of RIGDS technology applications are next (Ref 29):

- *Metal restoration and sealing:* engine blocks, castings, molds and dies, weld seams, auto body repair, refrigeration equipment, heat exchangers, cryogenic equipment
- *Thermal barriers:* aluminum piston heads, manifolds, disc brakes, aircraft engine components
- *Thermal dissipation:* copper or aluminum coatings on heat sinks for microelectronics
- *Soldering priming:* microelectronics components
- *Anti-stick properties:* deposits impregnated with release agents such as PTFE or silicone
- *Localized corrosion protection:* zinc or aluminum deposits on affected helms, weldments or other joints in which the original protective layer on the base material has been affected by the manufacturing process

However, much more scientific research is needed to better understand and optimize the RIGDS process so that its applicability can be extended into fields, where existing practices have limitations.

6. Conclusions

Experiments of both phenomenological and microstructural analyses of air GDS of the powder mixtures injected in the diverging part of a supersonic nozzle were performed. The results are summarized as follows:

- The GDS of powder mixtures results in the intensive process of powder microforging and the severe deformation of particles.
- The main characteristics of GDS such as deposition efficiency and average single pass thickness depend on the kinetics of adiabatic shear band formation following the Arrhenius flow law.

- Application of powder mixtures results in mechanical alloying during particle impact and consolidation.
- The particle cluster formation mechanism in the powder-laden jet was evaluated and it was shown that this process governs the impact powder consolidation features of RIGDS.

Acknowledgments

The work was supported by Centerline (Windsor) Limited. The authors thank Mr. Michael J. Beneteau for his support and continuing interest in the present work. The authors also acknowledge Dr. Julio Villafuerte for useful discussions and valuable contributions, and Mr. John Robinson for SEM examination.

References

1. A. Papyrin, Cold Spray Technology, *Advanced Materials & Processes,* 2001, **159**(9), p 49-51
2. J. Vlcek, L. Gimeno, H. Huber, and E. Lugscheider, A Systematic Approach to Material Eligibility for the Cold Spray Process, *Thermal Spray 2003: Advancing the Science & Applying the Technology*, B.R. Marple and C. Moreau, Ed., May 5-8, 2003 (Orlando, FL), ASM International, 2003, p 37-44
3. R.C. Dykhuizen, M.F. Smith, D.L. Gilmore, R.A. Neiser, X. Jiang, and S. Sampath, Impact of High Velocity Cold Spray Particles, *J. Therm. Spray Technol.,* 1999, **8**(4), p 559-564
4. C. Borchers, F. Gartner, T. Stoltenhoff, H. Assadi, and H. Kreye, Microstructural and Macroscopic Properties of Cold Sprayed Copper Coatings, *J. Appl. Phys.,* 2003, **93**(12), p 10064-10070
5. M. Grujicic, J.R. Saylor, D.E. Beasley, W.S. DeRosset, and D. Helfritch, Computational Analysis of the Interfacial Bonding between Feed-Powder Particles and the Substrate in the Cold-Gas Dynamic Spray Process, *Appl. Surf. Sci.,* 2003, **219**(3-4), p 211-227
6. A.P. Alkhimov, A.I. Gulidov, V.F. Kosarev, and N.I. Nestrovich, Specific Features of Microparticle Deformation Upon Impact on a Rigid Barrier, *J. Appl. Mech. Tech. Phys.,* 2000, **41**(1), p 204-209
7. D. Zhang, P.H. Shipway, and D.G. McCartney, Particle-Substrate Interactions in Cold Gas Dynamic Spraying, *Thermal Spray 2003: Advancing the Science & Applying the Technology,* B.R. Marple and C. Moreau, Ed., May 5-8, 2003 (Orlando, FL), ASM International, 2003, p 45-52
8. Chang-Jiu Li and Wen-Ya Li, Deposition Characteristics of Titanium Coating in Cold Spraying, *Surf. Coat. Technol.,* 2003, **167,** p 278-283
9. R.S. Lima, J. Karthikeyan, C.M. Kay, J. Lindemann, and C.C. Berndt, Microstructural characteristics of cold-sprayed nanostructured WC-Co coatings, *Thin Solid Films,* 2002, **416**(1-2), p 129-135
10. Chang Jiu Li, Guan-Jun. Yang, Xin-Chun Huang, and Wen-Ya Li, Formation of TiO_2 photocatalyst through Cold Spraying, *Thermal Spray 2004: Advances in Technology and Application,* ASM International, May 10-12, 2004 (Osaka, Japan), ASM International, 2004, p. 315-319
11. K. Sakaki and Y. Shimizi, Effect of the Increase in the Entrance Convergent Section Length of the Gun Nozzle on the High-Velocity Oxygen Fuel and Cold Spray Process, *J. Therm. Spray Technol.,* 2001, **10**(3), p 487-496
12. H. Assadi, F. Gartner, T. Stoltenhoff, and H. Kreye, Bonding Mechanism in Cold Gas Spraying, *Acta Mater.,* 2003, **51,** p 4379-4394
13. J.W. Walter, Numerical Experiments on Adiabatic Shear Band Formation in One Dimension, *Int. J. Plast.,* 1992, **8,** p 657-693
14. T.W. Wright, Steady Shearing in a Viscoplastic Solid, *J. Mech. Phys. Solids,* 1987, **35,** p 269-282
15. F.J. Zerilli and R.W. Armstrong, Dislocation Mechanics Based Constitutive Relations for Material Dynamics Calculations, *J. Appl. Phys.,* 1987, **61,** p 1816-1825
16. B. Dodd and Y. Bai, Width of Adiabatic Shear Bands Formed under Combined Stresses, *Materials Science and Technology,* 1989, **5**(6), p 557-559
17. T. Stoltenhoff, H. Kreye, and H.J. Richter, An Analysis of the Cold Spray Process and it's Coating, *J. Therm. Spray Technol.,* 2002, **11**(4), p 542-550
18. T.H. Van Steenkiste, J.R. Smith, R.E. Teets, J.J. Moleski, D.W. Gorkiewicz, R.P. Tison, D.R. Marantz, K.A. Kowalsky, W.L. Riggs, P.H. Zajchowski, B. Pilsner, R.C. McCune, and K.J. Barnett, Kinetic Spray Coatings, *Surf. Coat. Technol.,* 1999, **111,** p 62-71
19. R.G. Maev, E. Strumban, V. Leshchynsky, and M. Beneteau, Supersonic Induced Mechanical Alloy Technology and Coatings for Automotive and Aerospace Applications, *Cold Spray 2004: An Emerging Spray Coating Technology,* September 27-28, 2004 (Akron, Ohio), ASM International, 2004, Electronic
20. R.C. Dykhuizen and M.F. Smith, Gas Dynamic Spray Principles of Cold Spray, *J. Therm. Spray Technol.,* 1998, **7**(2), p 205-212
21. T.H. Steenkiste, J.R. Smith, and R.E. Teets, Aluminum Coatings via Kinetic Spray with Relatively Large Powder Particles, *Surf. Coat. Technol.,* 2002, **154,** p 237-252
22. T.W. Wright and R.C. Batra, The Initiation and Growth of Adiabatic Shear Bands, *Int. J. Plast.,* 1985, **1,** p 205-212
23. D.L. Zhang, Processing of Advanced Materials Using High-Energy Mechanical Milling Progress, *Mater. Sci.,* 2004, **49,** p 537-560
24. N. Hu and J.F. Molinari, Shear Bands in Dense Metallic Granular Materials, *J. Mech. Phys. Solids,* 2004, **52,** p 499-531
25. R.P. Flemming, W.E. Olmstead, and S.H. Davis, Shear Localization with an Arrhenius Flow Law, *J. Appl. Math.,* 2000, **60**(6), p 1867-1886
26. U.F. Kochs, A.S. Argon, and M.F. Ashby, *Thermodynamics and Kinetics of Slip,* Pergamon Press, Oxford, 1975
27. R.C. Senior and J.R. Grace, Integrated Particle Collision and Turbulent Diffusion Model for Dilute Gas-Solid Suspensions, *Powder Technol.,* 1998, **96**(1), p 48-78
28. D. Eskin and S. Voropaev, An Engineering Model of Particulate Friction in Accelerating Nozzles, *Powder Technol.,* 2004, **145**(3), p 203-212
29. Julio Villafuerte, Cold Spray: A New Technology, *Welding J,* 2005, **84**(5), p 24-29